Paul Brian Moore and Takaharu Araki

Contribution from the Department of the Geophysical Sciences, The University of Chicago, Chicago, Illinois 60637

A Mixed-Valence Solid-Solution Series: Crystal Structures of Phosphoferrite, $Fe^{II}_3(H_2O)_3[PO_4]_2$, and Kryzhanovskite, $Fe^{III}_3(OH)_3[PO_4]_2$

PAUL BRIAN MOORE* and TAKAHARU ARAKI

Received May 19, 1975 AIC50345K

A synthetic single crystal of $Fe^{II}_3(H_2O)_3[PO_4]_2$ (phosphoferrite) was studied in detail by three-dimensional x-ray diffractometry. The same crystal was heated in air to obtain the ferric end-member, $Fe^{III}_3(OH)_3[PO_4]_2$ (kryzhanovskite). Both compounds possess space group *Pbna*, $Z = 4$. For phosphoferrite, $a = 9.460$ (2), $b = 10.024$ (3), and $c = 8.670$ (2) Å; $R = 0.024$ ($R_w = 0.046$) for 1438 independent reflections. For kryzhanovskite, $a = 9.518$ (4), $b = 9.749$ (4), $c = 8.031$ (3) Å; $R = 0.036$ ($R_w = 0.055$) for 1316 reflections. X-ray diffraction data to $(\sin\theta)/\lambda = 0.75$ (Mo $K\alpha_1$ radiation) were collected on a Picker automated four-circle diffractometer and the structures were solved by Fourier and least-squares refinement techniques. Bond distance averages are Fe^{2+}–O = 2.16, 2.17 Å and P–O = 1.54 Å for phosphoferrite and Fe^{3+}–O = 2.01, 2.04 Å and P–O = 1.54 Å for kryzhanovskite. Polyhedral distortions in the two structures are compatible with an electrostatic valence bond strength model.

Introduction

The homologous series $Fe^{II}_3(H_2O)_n[PO_4]_2$ is a diverse example of a more general family of structure types, $M^{II}_3(H_2O)_n[TO_4]_2$, where M corresponds to octahedrally coordinated cations ($M^{2+} = Mg^{2+}$, Mn^{2+}, Fe^{2+}, Co^{2+}, Ni^{2+}, Zn^{2+}) and T to tetrahedrally coordinated small cations ($T^{5+} = P^{5+}$, As^{5+}, V^{5+}) in oxygen environments. In the structures investigated thus far, all oxygens associated with the tetrahedral anionic group and all water molecules are also bound to the octahedral cations. Their structures can be realized as progressive condensations of octahedral clusters with decreasing n. Setting ϕ = octahedral vertex, the general formula for these octahedral clusters can be written $M_3\phi_{8+n}$ and their classification is based in principle on the combinatorial topological solutions for fixed ratios in M and ϕ. The list of known compounds is rather impressive since many of the structure types include several isotypes. Of these compounds, the most studied are the n-aquo ferrous orthophosphates since they are well represented in mineralogical systems and it is these compounds that we shall discuss further.

For $n = 10$, no representative is as yet known. Such a compound would consist of insular octahedra and sets an upper limit on the degree of aquation. For $n = 8$, vivianite is the most familiar example and is based on octahedral edge-sharing dimers and insular octahedra.[1] The dimorph metavivianite[2] is rarely encountered and evidently has a small field of stability. Gautier[3] synthesized the $n = 6$ compound but evidence for its existence is not strong. To date, the most detailed attempt at synthesis of the homologues is by Mattievich,[4] who proceeded from synthetic vivaniate starting material and prepared other homologues in sealed capsules over a range of temperature, pressure, and pH and obtained crystals of the well-known $n = 4$ (ludlamite) and a hitherto unrecorded dimorph; $n = 3$ (phosphoferrite) and a possible dimorph; a poorly crystallized material of composition close to $n = 2$; the $n = 1$ compound which forms well-developed crystals; and the $n = 0$ dimorphs graftonite and sarcopside. Refined crystal structure determinations have been reported for ludlamite,[5] the $n = 1$ compound,[6] graftonite,[7,8] and sarcopside.[9,10]

The composition $Fe^{II}_3(H_2O)_3[PO_4]_2$ (phosphoferrite) and its oxidized equivalent $Fe^{III}_3(OH)_3[PO_4]_2$ (kryzhanovskite) are the subjects of this study. The mineralogical nomenclature shall be used to avoid ambiguity owing to polymorphism and difficulty in chemical nomenclature for such three-dimensional structures. Kryzhanovskite occurs as a natural mineral and its structure was determined.[11] However, as is often the case for minerals, the crystal exhibited extensive substitution by other cations and afforded an approximate composition $Fe^{III}_{1.8}Mn^{II}_{1.0}Ca_{0.1}Mg_{0.1}(OH)_{1.8}(H_2O)_{1.2}[PO_4]_2$. It was observed[12] that the $n = 3$ composition is capable of complete oxidation without destruction of the crystal structure but that all $n > 3$ compositions lead to amorphous and decomposed Fe^{3+} equivalents.[11] Consequently, detailed structure study of pure crystals of the $n = 3$ composition was most desirable.

Table I. Phosphoferrite and Kryzhanovskite Experimental Details

(A) Crystal Cell Data

	Phosphoferrite	Kryzhanovskite
a, Å	9.460 (2)	9.518 (4)
b, Å	10.024 (3)	9.749 (4)
c, Å	8.670 (2)	8.031 (3)
V, Å^3	822.2 (0.5)	745.2 (0.6)
$V/44$, Å^3	18.7	16.9
Space group	*Pbna*	*Pbna*
Z	4	4
Formula	$Fe^{II}_3(H_2O)_3[PO_4]_2$	$Fe^{III}_3(OH)_3[PO_4]_2$
ρ(calcd), g cm^{-3}	3.32	3.64
μ, cm^{-1}	58	64

(B) Intensity Measurements

Crystal size, mm	0.24 (∥*a*), 0.07 (∥*b*), 0.07 (∥*c*)
Crystal orientation	ϕ axis = [100]
Max $(\sin\theta)/\lambda$	0.75
Scan speed	2.0° min^{-1}
Base scan width	2.5°
Background counts	Stationary, 20 sec at beginning and end of scan
Radiation	Mo $K\alpha_1$ (λ 0.7926 Å), graphite monochromator
Independent F_o	1438 (phosphoferrite), 1316 (kryzhanovskite)

(C) Refinement of the Structure

	Phospho-ferrite	Kryzhan-ovskite
R	0.024	0.036
R_w	0.046	0.055
Scale factor	4.14 (1)	2.95 (1)
Goodness of fit	2.37	3.38

Experimental Procedure

Pure pale green crystals of the $n = 3$ compound (phosphoferrite) were synthesized by Dr. E. Mattievich, who employed hydrothermal synthesis starting with synthetic vivianite.[4] According to Dr. Mattievich, crystals can be grown in good yield between pH 5 and pH 6 and between 100 and 200°C. A 40-hr run afforded well-developed prisms whose morphology is shown in Figure 1. We collected a three-dimensional single-crystal data set on a carefully selected crystal. A dual data set was then collected on the deep red ferric equivalent (kryzhanovskite) which was prepared by heating the same crystal in air at 180°C for 48 hr. Thus, we obtained self-consistent data pairs for the same crystal and note that the same

Table II. Phosphoferrite[a] and Kryzhanovskite[b] Atomic Coordinate Parameters[c]

	x	*y*	*z*		*x*	*y*	*z*
Fe(1)	0.00000	0.00000	0.00000	O(4)	0.14429 (15)	0.09993 (13)	0.12530 (14)
	0.00000	0.00000	0.00000		0.15816 (22)	0.08792 (23)	0.10917 (27)
Fe(2)	0.06348 (3)	0.09782 (2)	0.63668 (3)	OW(1)	−0.08684 (26)	0.25000	0.50000
	0.04838 (4)	0.11378 (4)	0.63693 (5)	OH(1)	−0.05246 (31)	0.25000	0.50000
P	0.20288 (5)	0.10670 (4)	0.29122 (5)	OW(2)	−0.02832 (14)	0.32797 (13)	0.14766 (15)
	0.20925 (7)	0.10570 (7)	0.28596 (9)	OH(2)	−0.02974 (23)	0.34471 (23)	0.15037 (26)
O(1)	0.21539 (14)	0.25627 (12)	0.33460 (16)	H(1)	−0.134	0.200	0.446
	0.21008 (20)	0.25961 (20)	0.33188 (28)		−0.163	0.250	0.500
O(2)	0.10316 (13)	0.03661 (14)	0.40657 (14)	H(2a)	−0.100	0.310	0.156
	0.11247 (21)	0.02965 (21)	0.41434 (26)		−0.131	0.311	0.158
O(3)	0.35040 (13)	0.04224 (13)	0.29614 (14)	H(2b)	0.023	0.268	0.133
	0.35969 (21)	0.04537 (21)	0.29859 (27)			Absent	

[a] Upper values. [b] Lower values. [c] Estimated standard errors in parentheses refer to the last digit.

extinction and geometrical corrections were applied to both sets.

Preliminary precession photographs and the morphological evidence supported the space group *Pbna*, $Z = 4$, for both compounds. Table I lists the experimental details in this study. Utilizing a Picker FACS-1 automated four-circle diffractometer, least-squares refinement of 24 high-angle reflections led to the cell parameters in Table I. These values are slightly larger (0.2%) than those previously reported,[12] the latter obtained by powder refinement employing Cu $K\alpha_1$ radiation. We note that both compounds are approximately dense-packed, with 18.7 Å^3/oxygen for phosphoferrite and 16.9 Å^3/oxygen for kryzhanovskite.

The crystal measured 0.25 × 0.07 × 0.07 mm along the three crystallographic axes. Owing to the small size, favorable geometry, and relatively low linear absorption coefficient ($\mu = 58$ cm^{-1}), the maximum deviation in symmetry-equivalent intensities was observed to be less than 4% and no absorption correction was applied. Estimated errors of the intensities (σI) were calculated from $\sigma I^2 = S + t^2B$ where S = peak scan counts, B = total background counts, and t = ratio of the peak to background times. The σI's were then directly converted to the estimated errors in the structure factors (σF) with the structure factor magnitudes ($|F_o|$) obtained by applying the standard Lorentz and polarization factors. For the reflections with $I < 2\sigma I$, we set $I = \sigma I$. For the $|F_o|$ data set, symmetry-equivalent (hkl) and ($hk\bar{l}$) reflections and their errors were averaged. The total nonequivalent reflections were 1438 for phosphoferrite and 1316 for kryzhanovskite. Of these, 103 for phosphoferrite and 81 for kryzhanovskite applied to reflections with $I < 2\sigma I$.

Structure Determination and Refinement

Programs used in determining the structure included MAP (Fourier synthesis, by T. Araki), LPABWT2 (data reduction, including error assignment, by T. Araki), FLMXLS (least-squares refinement with options for bond distances and bond angles, by T. Araki), a highly modified version of RFINE (by L. W. Finger), and ORFLS (by W. R. Busing, K. O. Martin, and H. A. Levy).

Approximate metal coordinates were obtained from the earlier study[11] on natural kryzhanovskite and these were used to interpret the Patterson syntheses, $P(uvw)$, of both crystals. The metal positions thus obtained afforded a β synthesis[13] from which all remaining nonhydrogen atoms were located. Four cycles of scale factor, s, ($F_o = sF_c$), and atomic coordinate parameter refinement followed by two cycles of full-matrix scale factor, atomic coordinate parameter, and anisotropic thermal vibration parameter refinement converged to $R = 0.024$ and 0.046 and $R_w = 0.036$ and 0.055 for phosphoferrite and kryzhanovskite, respectively, where

$$R = \frac{\Sigma ||F_o| - |F_c||}{\Sigma |F_o|}$$

$$R_w = \left[\frac{\Sigma w(|F_o| - |F_c|)^2}{\Sigma w F_o^2}\right]^{1/2}$$

The final cycle minimized $\sum w||F_o| - |F_c||^2$ where $w = \sigma F^{-2}$. The "goodness of fit", $S = \sum w||F_o| - |F_c||^2/(n - m)$ where n = number of independent F's and m = number of parameters, is 2.37 and 3.38 for phosphoferrite and kryzhanovskite, respectively.

We employed scattering curves[14] for Fe^{2+}, P^0, and O^- for both refinements, anomalous dispersion[15] corrections, f'', for Fe and P,

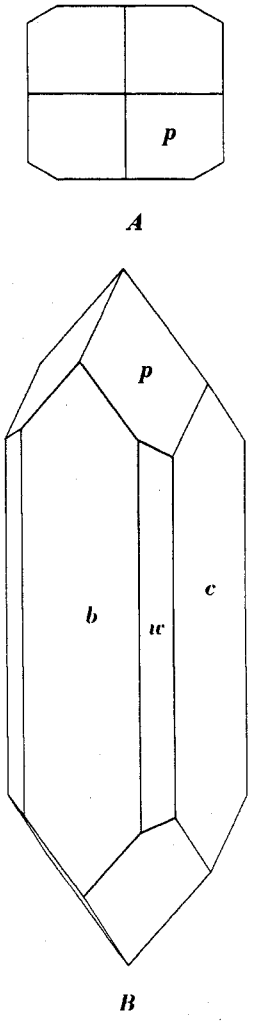

Figure 1. Typical development of synthetic phosphoferrite showing the forms c {001}, b {010}, w {021}, and p {111}: A, plan; B, clinographic projection.

and a secondary extinction[16] correction, c_0. The last value refined to $c_0 = 1.1\ (1) \times 10^{-6}$.

At this stage, difference syntheses were prepared with hopes that the hydrogen atom positions could be located. Although the hydrogen atoms were well resolved on the map for phosphoferrite, the map for kryzhanovskite was more diffuse. Nevertheless, we noted two prominent residuals which were at least twice the background level error and these were accepted as the hydrogen atom positions.

Estimated standard errors in distances were computed from the errors in atomic coordinate parameters only, since the errors in cell constants are negligible (maximum ±0.0000 (4)/Å).

Owing to the relatively dense structure of the two compounds and the presence of heavy atoms, these hydrogen atom coordinates were not included in the refinement. Atomic coordinate parameters for

Table III. Phosphoferrite[a] and Kryzhanovskite[b] Anisotropic Thermal Vibration Parameters ($\times 10^4$)[c]

Atom	β_{11}	β_{22}	β_{33}	β_{12}	β_{13}	β_{23}
Fe(1)	24.9	14.9	22.6	−2.6	−7.4	−0.2
	(3)	(3)	(4)	(2)	(3)	(5)
	5.9	24.7	37.8	−1.3	−4.8	3.5
	(6)	(6)	(8)	(4)	(5)	(5)
Fe(2)	21.4	17.3	21.3	5.0	−0.1	1.9
	(3)	(3)	(4)	(2)	(2)	(2)
	7.8	21.2	37.6	3.5	2.1	2.5
	(5)	(5)	(7)	(2)	(3)	(3)
P	12.2	13.4	17.9	−0.8	−0.5	0.6
	(4)	(4)	(5)	(3)	(3)	(3)
	3.6	17.9	33.5	0.3	−0.1	0.6
	(6)	(6)	(10)	(4)	(5)	(5)
O(1)	20.4	14.3	37.6	−0.2	0.7	4.6
	(11)	(10)	(15)	(9)	(10)	(9)
	2.6	15.9	55.5	2.2	−0.1	4.9
	(15)	(15)	(29)	(13)	(18)	(17)
O(2)	20.3	24.6	23.1	−6.8	−3.3	1.5
	(11)	(11)	(13)	(8)	(10)	(9)
	7.0	21.3	38.9	−3.4	−5.4	1.0
	(18)	(17)	(26)	(14)	(17)	(17)
O(3)	15.4	22.9	35.8	6.1	−0.7	3.5
	(10)	(11)	(14)	(9)	(10)	(10)
	4.3	26.6	42.8	3.7	0.4	−1.3
	(16)	(17)	(29)	(14)	(17)	(18)
O(4)	26.8	28.9	19.7	−5.6	−4.3	−1.9
	(13)	(11)	(13)	(10)	(10)	(9)
	9.3	34.5	36.4	−3.2	−6.1	−2.5
	(18)	(18)	(28)	(15)	(18)	(18)
OW(1)	44.2	30.5	55.3	0	0	8.4
	(21)	(18)	(26)			(16)
OH(1)	11.8	28.2	50.1	0	0	−5.6
	(27)	(26)	(43)			(27)
OW(2)	22.4	16.6	33.1	−3.1	−1.0	−0.4
	(11)	(10)	(14)	(9)	(10)	(9)
OH(2)	8.8	25.9	40.5	−3.5	−4.3	1.3
	(17)	(18)	(27)	(14)	(17)	(18)

[a] Upper values. [b] Lower values. [c] Coefficients in $\exp[-(\beta_{11}h^2 + \beta_{22}k^2 + \beta_{33}l^2 + 2\beta_{12}hk + 2\beta_{13}hl + 2\beta_{23}kl)]$.

both compounds are presented in Table II, the anisotropic thermal vibration parameters in Table III, the crystallographic orientation of their principal vibration directions in Table IV, and pertinent bond distances and angles in Table V.

Anomalies in the Scale Factors and Thermal Vibrations

It is appropriate to remark here that the scale factor, s, refined to 4.14 (1) and 2.95 (1) for phosphoferrite and kryzhanovskite, respectively. Since the conditions throughout data collection were effectively identical and since the same starting crystal was used in both studies, we feel that the attenuation of intensities by about 29% for kryzhanovskite arises from differences in mosaicity and degree of homogeneous domains between the two crystals. Evidence is accumulating through optical study that the progressive oxidation of phosphoferrite crystals is not homogeneous and random throughout the crystal but proceeds in part as local patches which follow along joints and cracks so that the crystal defects in the ferric end-member are different from those of the ferrous starting material. The principal indexes of refraction and orientation of the optical indicatrices have been reported elsewhere.[12]

Further support for mosaicity differences between the two crystals can be seen in Table IV. Although the thermal vibration ellipsoids are slightly oblate in phosphoferrite, they are extremely so in kryzhanovskite. In addition, the direction of compression is strongly preferential in the latter compound, ranging from 0 to 18° from the a axis. Inspection of the structure shows that the preferred orientation cannot arise from bonding effects but probably arises from preferred orientation of mosaic blocks, with maximal disorder in the plane parallel to {100}. This, in effect, leads to a dilation of the elliptical cross section in the {100} plane. A diminution in the root-mean-square amplitude μ_2, approximately normal to the sheets, arises from the greater bond strength of Fe^{3+}–O with respect to Fe^{2+}–O. Indeed, the rms displacement for oxygen in the dense ferric oxide hematite ranges from 0.04 to 0.10 while, in ferrous oxide compounds, the range is similar to that found in phosphoferrite. From these observations, it is tempting to propose that diffusion of oxygen and hydrogen during the course of oxidation proceeds along, but not between, the {100} planes, i.e., the planes of approximate oxygen dense-packing.

Description of the Structure

The structure type which embraces both phosphoferrite and kryzhanovskite is based on sheets of corner- and edge-linked oxygen octahedra which are oriented parallel to {100} at $x \approx 0$ and $1/2$ (Figure 2). The phosphate tetrahedra at $x \approx 1/4$ and $3/4$ are situated between these symmetry-equivalent

Table IV. Phosphoferrite and Kryzhanovskite Parameters for the Ellipsoids of Vibration[a]

Phosphoferrite							Kryzhanovskite						
Atom	i	μ_i	θ_{ia}	θ_{ib}	θ_{ic}	B, Å^2	Atom	i	μ_i	θ_{ia}	θ_{ib}	θ_{ic}	B, Å^2
Fe(1)	1	0.116	147	80	58	0.72	Fe(1)	1	0.118	99	52	39	0.71
	2	0.078	58	60	46			2	0.048	11	88	80	
	3	0.089	98	31	120			3	0.104	85	38	127	
Fe(2)	1	0.109	41	50	82	0.70	Fe(2)	1	0.114	81	65	27	0.69
	2	0.080	56	137	67			2	0.056	167	77	86	
	3	0.091	69	103	155			3	0.100	80	28	116	
P	1	0.085	104	44	49	0.50	P	1	0.105	90	84	6	0.52
	2	0.073	15	76	84			2	0.013	1	91	90	
	3	0.081	95	49	139			3	0.093	89	6	96	
O(1)	1	0.122	87	75	15	0.81	O(1)	1	0.136	89	80	10	0.71
	2	0.082	94	164	75			2	0.032	9	99	89	
	3	0.096	4	94	92			3	0.086	81	14	100	
O(2)	1	0.122	122	35	78	0.80	O(2)	1	0.115	103	76	20	0.69
	2	0.082	36	66	65			2	0.050	15	79	79	
	3	0.094	75	67	152			3	0.102	97	18	106	
O(3)	1	0.121	79	54	31	0.85	O(3)	1	0.119	93	114	24	0.76
	2	0.074	28	117	83			2	0.041	171	81	89	
	3	0.110	65	48	127			3	0.114	99	154	114	
O(4)	1	0.128	123	33	88	0.90	O(4)	1	0.130	85	169	81	0.86
	2	0.081	67	77	27			2	0.058	18	82	74	
	3	0.107	42	60	117			3	0.112	73	97	161	
OW(1)	1	0.151	90	63	27	1.49	OH(1)	1	0.133	90	119	29	0.93
	2	0.117	90	153	63			2	0.074	0	90	90	
	3	0.141	180	90	90			3	0.111	90	151	119	
OW(2)	1	0.113	100	89	10	0.82	OH(2)	1	0.118	103	59	34	0.78
	2	0.087	59	31	86			2	0.059	13	80	81	
	3	0.105	148	59	99			3	0.111	93	33	123	

[a] i = ith principal axis; μ_i = rms amplitude; θ_{ia}, θ_{ib}, θ_{ic} = angles (deg) between the ith principal axis and the cell axes a, b, and c.

Table V. Phosphoferrite and Kryzhanovskite Polyhedral Interatomic Distances and Angles†

PHOSPHOFERRITE

Fe(1)

2 Fe(1) - O(4)^{iv}	2.012(2)Å	
2 -OW(2)^{iv}	2.164(2)	
2 - O(3)^{i}	2.304(2)	
average	2.160Å	
		O–Fe(1)–O′
2 OW(2)^{iv} - O(3)^{ii}	2.772(3)*	76.6(1)°
2 O(4) - O(3)^{iii}	2.920(3)	84.9(1)
2 OW(2)^{iv} - O(4)^{iv}	2.945(3)	89.6(1)
2 O(4) -OW(2)^{iv}	2.965(3)	90.4(1)
2 O(4)$_{iv}$ - O(3)^{ii}	3.190(3)	95.1(1)
2 OW(2)^{iv} O(3)^{i}	3.507(3)	103.4(1)
average	3.050	90.0

P

P-O(3)	1.539(2)	
-O(4)	1.543(2)	
-O(2)	1.544(2)	
-O(1)	1.550(2)	
average	1.544	
		O–P–O′
O(1)-O(4)	2.490(3)	107.23(7)°
O(3)-O(4)	2.516(3)	109.46(7)
O(1)-O(3)	2.519(3)	109.28(7)
O(1)-O(2)	2.523(3)	109.25(8)
O(2)-O(3)	2.528(3)	110.19(7)
O(2)-O(4)	2.550(3)	111.37(8)
average	2.521	109.46

HYDROGEN DISTANCES

H(1)

2 H(1) -OW(1)$_{i}$	0.82
2 H(1)···O(3)^{i}	2.63
sum	3.45
2 OW(1)···O(3)^{i}	3.359(4)

KRYZHANOVSKITE

Fe(1)

2 Fe(1) - O(4)$_{iv}$	1.941(3)	
2 -OH(2)^{iv}	1.957(3)	
2 - O(3)^{i}	2.144(3)	
average	2.014	
		O–Fe(1)–O′
2 OH(2)^{iv} - O(3)^{ii}	2.572(4)*	77.5(1)°
2 OH(2)^{iv} - O(4)^{ii}	2.688(4)	87.2(1)
2 O(4) - O(3)^{ii}	2.817(4)	87.1(1)
2 O(4) -OH(2)^{iv}	2.824(4)	92.8(1)
2 O(4)$_{iv}$ - O(3)^{i}	2.965(4)	92.9(1)
2 OH(2)^{iv} - O(3)^{i}	3.199(4)	102.5(1)
average	2.844	90.0

P-O(4)	1.511(3)	
-O(1)	1.545(3)	
-O(3)	1.551(3)	
-O(2)	1.569(3)	
average	1.544	
		O–P–O′
O(3)-O(4)	2.483(4)	108.37(12)°
O(1)-O(4)	2.499(4)	109.71(13)
O(1)-O(2)	2.515(4)	107.76(12)
O(2)-O(3)	2.535(4)	108.65(12)
O(1)-O(3)	2.542(4)	110.35(11)
O(2)-O(4)	2.553(4)	111.99(12)
average	2.521	109.47

HYDROGEN DISTANCES

H(1)

1 H(1) -OW(1)$_{i}$	1.05
1 H(1)···O(3)^{i}	3.13
sum	4.18
1 OW(1)···O(3)^{i}	3.229(4)

PHOSPHOFERRITE

Fe(2)

Fe(2) - O(1)$^{iv}_{iii}$	2.066(2)	
- O(2)^{iii}	2.108(2)	
- O(2)$_{ii}$	2.121(2)	
- O(3)^{ii}	2.132(2)	
-OW(2)^{iv}	2.192(2)	
-OW(1)	2.399(3)	
average	2.170	
		O–Fe(2)–O′
O(2)$_{ii}$ - O(2)^{iii}	2.641(3)*	77.3(1)°
O(3)^{ii} -OW(2)^{iv}	2.772(3)*	79.7(1)
OW(2)^{iv} - O(1)^{iv}	2.908(3)	86.1(1)
OW(1)$_{ii}$ - O(2)^{iii}	2.909(4)	79.9(1)
O(3)^{ii} - O(2)^{iii}	2.968(3)	88.9(1)
OW(1)$_{ii}$ - O(2)^{iv}	2.989(4)	82.8(1)
O(3)^{iii} - O(1)^{iv}	3.145(3)	97.0(1)
O(2)^{iii} -OW(2)^{iv}	3.149(3)	94.2(1)
OW(1) - O(1)^{iv}	3.199(4)	91.2(1)
OW(1)$_{iv}$ -OW(2)^{iv}	3.202(4)	88.3(1)
O(1)^{ii} - O(2)	3.236(3)	101.2(1)
O(3)^{ii} - O(2)	3.496(3)	110.6(1)
average	3.051	89.8

HYDROGEN DISTANCES

H(2)

H(2a) -OW(2)$_{i}$	0.71
H(2a) O(1)^{i}	1.83
sum	2.54
OW(2) O(1)^{i}	2.533(3)

H(2b) -OW(2)	0.78
H(2b)···O(4)	2.04
sum	2.82
OW(2)···O(4)	2.816(3)

KRYZHANOVSKITE

Fe(2)

Fe(2) -OH(2)^{iv}	1.906(3)	
-OH(1)$_{iv}$	1.973(3)	
- O(1)^{iv}	1.989(3)	
- O(2)$_{iv}$	2.059(3)	
- O(2)$_{iii}$	2.114(3)	
- O(3)^{ii}	2.204(3)	
average	2.041	
		O–Fe(2)–O′
O(3)^{ii} -OH(2)^{iv}	2.572(4)*	77.1(1)°
O(2) - O(2)^{iii}	2.610(4)*	77.4(1)
OH(1)$_{iv}$ - O(2)$_{iv}$	2.748(4)	85.9(1)
OH(2)^{iv} - O(1)^{iv}	2.832(4)	93.3(1)
OH(1) - O(1)^{iv}	2.842(4)	91.7(1)
OH(1)$_{iii}$ - O(2)^{iv}	2.869(4)	89.1(1)
O(2)$_{ii}$ -OH(2)^{iii}	2.892(4)	91.9(1)
O(3)^{ii} - O(2)^{iv}	2.956(4)	86.4(1)
OH(1)^{iv} -OH(2)^{iv}	2.964(4)	99.6(1)
O(1)^{iv} - O(2)$_{iv}$	3.039(4)	97.3(1)
O(3)^{ii} - O(1)^{iv}	3.050(4)	93.2(1)
O(3)^{ii} - O(2)	3.182(4)	96.5(1)
average	2.880	89.9

HYDROGEN DISTANCES

H(2)

H(2a) -OW(2)$_{i}$	0.99
H(2a)···O(1)^{i}	1.56
sum	2.55
OW(2)···O(1)^{i}	2.541(4)

H(2b) is absent

OW(2)···O(4)	3.094

†Estimated standard deviations refer to the last digit.

*Fe–Fe oxygen octahedral shared edges. i = 1/2+, +, 1/2-; ii = 1/2-, -, 1/2+; iii = -, -, -; iv = +, 1/2-, - applied to atom coordinates in Table 2.

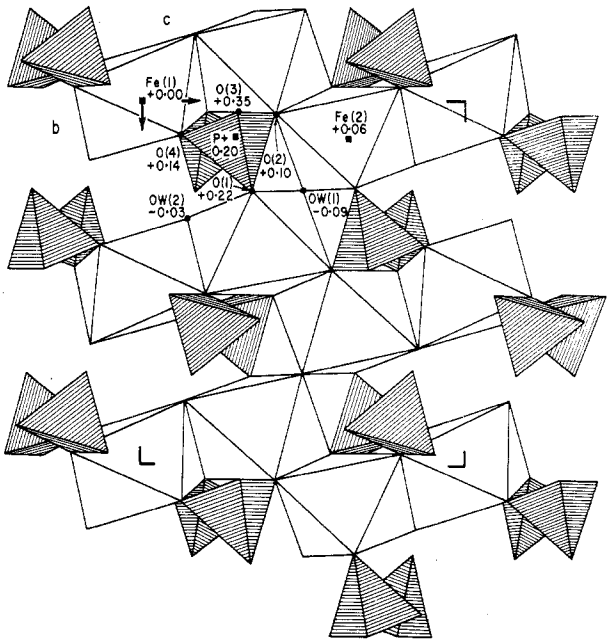

Figure 2. Polyhedral diagram of the phosphoferrite crystal structure down the *a* axis. Heights are given as fractional coordinates in *x* and the atoms designated correspond to Table II. The slab is positioned where $-1/2 < x < +1/2$. The octahedral sheet is unshaded and the linking $[PO_4]$ tetrahedra are ruled.

octahedral sheets and link to them by corner sharing. As a result, the structure is a rather rigid framework of octahedra and tetrahedra and the crystals exhibit no good cleavage direction.

Components of the octahedral sheet are particularly interesting. Octahedral edge-sharing trimers occur (Fe(2)–Fe(1)–Fe(2)) with point symmetry $\bar{1}$, the shared edge pairs being OW(2)–O(3)^{ii}. The trimers further link to symmetry-equivalent trimers via the edges O(2)–O(2)^{iii} to form a staggered octahedral edge-sharing chain which is oriented parallel to the [001] axial direction. This is the only continuous edge-sharing component in the structure. Symmetry-equivalent chains are further linked by corner-sharing at OW(1) which is situated on the twofold rotors in the structure. The pertinent nonequivalent metal–metal separations are Fe(1)–Fe(2) = 3.353, 3.154 Å, Fe(2)–Fe(2)^{iii} = 3.302, 3.257 Å, and Fe(2)–Fe(2)^{iv} = 3.864, 3.448 Å for phosphoferrite and kryzhanovskite, respectively. The first two pairs are across shared octahedral edges. Foreshortening of the distances is offset by the strong cation–cation repulsions for the ferric member. In the absence of such repulsion, the separations would be about 3.05 and 2.86 Å for phosphoferrite and kryzhanovskite, respectively, i.e., the octahedral edge averages. Evidently, these distortions, prominent in the ferric compound, are compensated by a decrease of 0.42 Å for the Fe(2)–Fe(2)^{iv} distance across the shared corner.

Three independent hydrogen atoms in general positions (Table II) were located for phosphoferrite and these results confirm the proposed hydrogen bond distribution in an earlier study.[11] Two of these, OW(1)···O(3)^{i} with a distance of 3.36 Å and OW(2)···O(4) with a 2.82-Å distance, bridge across gaps within a sheet. The third, OW(2)···O(1)^{i} with a 2.53-Å distance, links between sheets. In kryzhanovskite, the H(2b) atom is absent and the bond OW(2)···O(4) is missing. Evidently, the shorter (thus stronger) OW(2)···O(1)^{i} bond is conserved throughout oxidation of the phosphoferrite crystal (in kryzhanovskite, its distance is 2.54 Å). A curious feature for the OH(1)···O(3)^{i} bond occurs in kryzhanovskite. Since OW(1) has an equipoint rank number half that of the other oxygen atoms, loss of one hydrogen atom should lead to a statistical half-occupancy at the hydrogen general position. Instead, the H(1) atom is located *on* the twofold rotor, achieving full occupancy of a site. Consequently, O(3) receives half of a relatively weak hydrogen bond. In phosphoferrite, the OW(1) contribution is relatively weak and is further exemplified by the wide O(3)^{vi}–OW(1)–O(3)^{i} = 159.6° angle. For OW(2), this angle is close to the ideal tetrahedron, with O(4)–OW(2)–O(1)^{i} = 109.2°.

The evidence for the shift of H(1) from a general equipoint set to the special set rests on the difference synthesis for kryzhanovskite. The residual density at the H(1) position in that crystal was observed to be absent on the phosphoferrite difference map. Conversely, the general H(1) position in phosphoferrite was missing in kryzhanovskite.

Perhaps the most interesting aspect of the structure is found to the relative polyhedral distortions for the two end-members. The average Me–O distances are Fe(1)–O = 2.16, 2.01 Å, Fe(2)–O = 2.17, 2.04 Å, and P–O = 1.54, 1.54 Å for phosphoferrite and kryzhanovskite, respectively. These averages agree well with those based on recently proposed[17] empirical effective radii: Fe^{2+}–O = 2.18 Å, Fe^{3+}–O = 2.04 Å, P^{5+}–O = 1.57 Å. Table V lists the polyhedral distances as increasing values, to facilitate discussion about distortions in the two structures. The shortest octahedral edge distances, namely, O(2)–O(2)^{iii}, O(3)^{ii}–OW(2)^{iv}, and O(3)^{ii}–OH(2)^{iv}, are those shared between octahedra. It is noticed, however, that the relative Me–O distances do not correspond at all between the two compounds. This is especially apparent for the P–O distances even though the polyhedral averages are identical in both structures. An even more striking difference is noted between the Fe(2)–OW distances and the isotypic Fe(2)–OH distances: in phosphoferrite these are the longest but in kryzhanovskite they are the shortest polyhedral distances.

The explanation lies in the electrostatic valence bond[18] sum deviations of cations about anions and the effect of these deviations on the individual bond distances. The bond strength (s) is defined as the formal charge of the cation divided by its coordination number. The O–H donor bond (herein labeled H_d) is ascribed $s = 5/6$ and the O–H···O acceptor bond (herein labelled H_a) is given $s = 1/6$, as proposed by Baur[19] on the grounds of empirical studies on oxysalt hydrates. It is seen in Table VI that the bond strength sums, p_x, deviate from saturation (2.00) in the same direction as the deviation of individual bond distances from the polyhedral averages, with undersaturated anions possessing shorter than average and oversaturated anions longer than average distances. The only apparent contradiction appears for OW(2) in phosphoferrite: here, the deviation in Fe^{2+}–O bond distances is not as severe as predicted by the bond strength sum model. Since both OW(2)···O bonds are relatively strong, the corresponding acceptor bonds probably are stronger than $s = 1/6$ and the donor bonds would each have strengths less than $s = 5/6$. The generally good agreement between the polyhedral distortions and the electrostatic bond strength sum model adds further support to the assignments of hydrogen bonds and provides, to our knowledge, the only example of such a study on two end-members of a mixed-valence series.

Discussion

Although it is clearly established that two end-members of a mixed-valence series can exist without severe damage to the structure, the question remains as to why similar series do not exist for the homologues with $n > 3$. It has been suggested[11] that the more highly aquated homologues would be electrostatically unstable as ferric end-members and during the process of oxidation would decompose. In ludlamite ($n = 4$), for example, each of the water molecules is bonded to two Fe^{2+} cations. This means that for the ferric end-member,

Table VI. Phosphoferrite and Kryzhanovskite Electrostatic Valence Balances of Cations about Anions

Anions	Coordinating cations	p_x	Comments[a]
	Phosphoferrite		
O(1)	$H(2a)_a$ + P + Fe(2)	1.75	P (0), Fe(2) (very −)
O(2)	P + 2Fe(2)	1.92	P (0), Fe(2) (−), Fe(2) (−)
O(3)	$H(1)_a$ + P + Fe(1) + Fe(2)	2.08	P (0), Fe(1) (very +), Fe(2) (−)
O(4)	$H(2b)_a$ + P + Fe(1)	1.75	P (0), Fe(1) (very −)
OW(1)	$2H(1)_d$ + 2Fe(2)	2.33	Fe(2) (very +)
OW(2)	$H(2a)_d$ + $H(2b)_d$ + Fe(1) + Fe(2)	2.33	Fe(1) (0), Fe(2) (+)
	Kryzhanovskite		
O(1)	$H(2a)_a$ + P + Fe(2)	1.92	P (0), Fe(2) (−)
O(2)	P + 2Fe(2)	2.25	P (+), Fe(2) (+), Fe(2) (+)
O(3)	$^1/_2H(1)_a$ + P + Fe(1) + Fe(2)	2.33	P (0), Fe(1) (very +), Fe(2) (very +)
O(4)	P + Fe(1)	1.75	P (−), Fe(1) (−)
OH(1)	$H(1)_d$ + 2Fe(2)	1.83	Fe(2) (−)
OH(2)	$H(2a)_d$ + Fe(1) + Fe(2)	1.83	Fe(1) (−), Fe(2) (very −)

[a] Individual bond distances within 0.03 Å of the polyhedral average are (0), within 0.03 and 0.10 Å are (+, −), and greater or less than 0.10 Å are (very +, very −).

$Fe^{III}_3(OH)_3(H_2O)[PO_4]_2$, one water molecule must be bound to two Fe^{3+} cations. Such an arrangement has not heretofore been recorded for a mineral structure, presumably because it is electrostatically very unstable (p_x = 2.67). In such a structure, the water molecule is probably split off and the crystal undergoes topological rearrangement of the octahedra. At temperatures below 200°C, the kinetics of rearrangement are apparently far too slow for any recrystallization to take place and the quenched product is amorphous to x radiation. For vivianite, the situation is just as extreme since each water molecule is bonded to only one Fe^{2+} cation. Thus, in the composition $Fe^{III}_3(OH)_3(H_2O)_5[PO_4]_2$, three OH^- anions will each be bonded to only one Fe^{3+} cation yielding another electrostatically unstable arrangement (p_x = 1.33). It appears that only phosphoferrite has all of the desirable properties (Fe^{2+}:H_2O = 1:1, two Fe^{2+} ions bonded to each H_2O) to ensure stability throughout oxidation.

Are intermediate compositions stable for all Fe^{2+}:(Fe^{2+} + Fe^{3+}) ratios, and, if so, is the (Fe^{2+}, Fe^{3+}) pair a solid solution? It is unlikely that such a problem can be tackled by a simple x-ray diffraction experiment since such results are *averaged* over the entire crystal. On electrostatic grounds, it is plausible that oxidation of the Fe^{2+} proceeds in a cooperative basis, that is, $2Fe^{2+}(H_2O) \rightarrow 2Fe^{3+}(OH)^- + H_2$ where the two metals are bound to the same water molecule. On the other hand, other units, undersaturated and oversaturated with respect to the cations, have been found in mineralogical systems:[10,21] $Fe^{3+}{}_3O^{2-}$, $Fe^{3+}{}_3(OH)^-$, $Fe^{3+}{}_2Fe^{2+}(OH)^-$, $Fe^{2+}Fe^{3+}(OH)^-$. Their relative stability can be attested by the fact that the mineral crystals were intact over the order of 10^6 years! Units like $Fe^{2+}Fe^{2+}(OH)^-$, $Fe^{3+}Fe^{3+}(H_2O)$, and $Fe^{2+}Fe^{3+}(H_2O)$ have never been found in mineral crystals and, for reasons stated above, are predicted to be unstable. On these grounds, all intermediate compositions for phosphoferrite should be stable since they would involve combinations like Fe^{2+} $Fe^{2+}(H_2O)$, $Fe^{2+}Fe^{3+}(OH)^-$ and $Fe^{3+}Fe^{3+}(OH)^-$. The most compelling evidence is the easy synthesis of the ferric end-member: if some intermediate composition were unstable, the final product would be essentially amorphous.

One intriguing question remains and concerns the intermediate composition $Fe^{2+}{}_2Fe^{3+}(OH)(H_2O)_2[PO_4]_2$. Is the ordering scheme Fe(1) = Fe^{3+}, Fe(2) = Fe^{2+}; Fe(1) = Fe^{2+}, Fe(2) = $Fe^{2+}{}_{0.5}Fe^{3+}{}_{0.5}$; Fe(1) = Fe(2) = $Fe^{2+}{}_{0.67}Fe^{3+}{}_{0.33}$, or some more complicated scheme? The only hint favoring Fe(1) = Fe^{3+} is found in the structure analysis of natural kryzhanovskite, where polyhedral distances suggest 4 Fe(1) = $Fe^{3+}{}_{4.0}$ and 8 Fe(2) = $Mn^{2+}{}_{3.7}Fe^{3+}{}_{3.1}Ca^{2+}{}_{0.4}\square_{0.8}$. It suggests that the site at the inversion center is favored by smaller more highly charged cations. For the pure iron compounds, however, this question can only be settled by direct attempt at hydrothermal synthesis of that intermediate composition.

Acknowledgment. It is a pleasure to thank Dr. Enrico Mattievich of Centro Brasileiro de Pesquisas Fisicas (Rio de Janeiro) for donation of the single crystals. This study was supported by National Science Foundation Grant GA-40543 and a Materials Research Laboratory grant (NSF) awarded to The University of Chicago.

Registry No. $Fe^{II}_3(H_2O)_3[PO_4]_2$, 54864-45-8; $Fe^{III}_3(OH)_3[PO_4]_2$, 55071-02-8.

Supplementary Material Available: Structure factor tables (20 pages). Ordering information is given on any current masthead page.

References and Notes

(1) H. Mori and T. Ito, *Acta Crystallogr.*, **3**, 1 (1950).
(2) C. Ritz, E. J. Essene, and D. R. Peacor, *Am. Mineral.*, **59**, 896 (1974).
(3) A. Gautier, *Bull. Soc. Chim. Fr.*, **9**, 884 (1893).
(4) E. Mattievich, Doctoral Dissertation, Centro Brasileiro de Pesquisas Fisicas, Rio de Janeiro, 1974.
(5) S. C. Abrahams and J. L. Bernstein, *J. Chem. Phys.*, **44**, 2223 (1966).
(6) P. B. Moore and T. Araki, *Am. Mineral.*, **60**, 454 (1975).
(7) C. Calvo, *Am. Mineral.*, **53**, 742 (1968).
(8) E. Kostiner and J. R. Rea, *Inorg. Chem.*, **13**, 2876 (1974).
(9) P. B. Moore, *Am. Mineral.*, **57**, 24 (1972).
(10) Yu. K. Kabalov, M. A. Simonov, O. B. Yakubovich, N. A. Yamnova, and N. V. Belov, *Sov. Phys.—Dokl. (Engl. Transl.)*, **18**, 362 (1973).
(11) P. B. Moore, *Am. Mineral.*, **56**, 1 (1971).
(12) P. B. Moore, *Nature (London)*, **251**, 305 (1974).
(13) G. N. Ramachandran and R. Srinivasan, "Fourier Methods in Crystallography", Wiley-Interscience, New York, N.Y., 1970, p 96.
(14) D. T. Cromer and J. B. Mann, *Acta Crystallogr., Sect. A*, **24**, 321 (1968).
(15) D. T. Cromer and D. Liberman, Report LA-4403, UC-34, Los Alamos Scientific Laboratory, University of California, Berkeley, Calif., 1970.
(16) W. H. Zachariasen, *Acta Crystallogr., Sect. A*, **24**, 425 (1968).
(17) R. D. Shannon and C. T. Prewitt, *Acta Crystallogr., Sect. B*, **25**, 925 (1969).
(18) L. Pauling, "The Nature of the Chemical Bond", 3rd ed., Cornell University Press, Ithaca, New York, N.Y., 1960, p 548.
(19) W. H. Baur, *Trans. Am. Crystallogr. Assoc.*, **6**, 129 (1970).
(20) P. B. Moore, *Neues Jahrb. Mineral. Monatsh.* 39 (1970).
(21) P. B. Moore, *Am. Mineral.*, **57**, 397 (1972).